A LETTERS JOURNAL EXPLORING THE FRONTIERS OF PHYSICS

OFFPRINT

The effective flux through a thin-film composite membrane

M. BRUNA, S. J. CHAPMAN and G. Z. RAMON

EPL, **110** (2015) 40005

OVER
560,000
full text downloads in 2013

24 DAYS
average accept to online publication in 2013

10,755
citations in 2013

"We greatly appreciate the efficient, professional and rapid processing of our paper by your team."

Cong Lin
Shanghai University

Six good reasons to publish with EPL

We want to work with you to gain recognition for your research through worldwide visibility and high citations. As an EPL author, you will benefit from:

1. **Quality** – The 50+ Co-editors, who are experts in their field, oversee the entire peer-review process, from selection of the referees to making all final acceptance decisions.
2. **Convenience** – Easy to access compilations of recent articles in specific narrow fields available on the website.
3. **Speed of processing** – We aim to provide you with a quick and efficient service; the median time from submission to online publication is under 100 days.
4. **High visibility** – Strong promotion and visibility through material available at over 300 events annually, distributed via e-mail, and targeted mailshot newsletters.
5. **International reach** – Over 2600 institutions have access to EPL, enabling your work to be read by your peers in 90 countries.
6. **Open access** – Articles are offered open access for a one-off author payment; green open access on all others with a 12-month embargo.

Details on preparing, submitting and tracking the progress of your manuscript from submission to acceptance are available on the EPL submission website **www.epletters.net**.

If you would like further information about our author service or EPL in general, please visit **www.epljournal.org** or e-mail us at **info@epljournal.org**.

EPL is published in partnership with:

European Physical Society | Società Italiana di Fisica | EDP Sciences | IOP Publishing

A Letters Journal Exploring the Frontiers of Physics

May 2015

EPL, **110** (2015) 40005
doi: 10.1209/0295-5075/110/40005

www.epljournal.org

The effective flux through a thin-film composite membrane

M. Bruna[1(a)], S. J. Chapman[1] and G. Z. Ramon[2]

[1] *Mathematical Institute, University of Oxford - OX2 6GG Oxford, UK*
[2] *Department of Civil & Environmental Engineering, Technion - Israel Institute of Technology Haifa 32000, Israel*

received 23 March 2015; accepted in final form 15 May 2015
published online 8 June 2015

PACS 02.30.Mv – Approximations and expansions
PACS 66.30.J- – Diffusion of impurities
PACS 82.45.Mp – Electrochemistry and electrophoresis: Thin layers, films, monolayers, membranes

Abstract – Composite membrane structures, used extensively in separation processes, comprise an ultra-thin selective polymer film cast over a porous support, whose pores partially obstruct transport out of the top film. Here, we model the composite as a finite thickness slab with a periodic array of circular absorbing patches in an otherwise reflective surface and study the effective transport properties of the composite. We obtain an analytical approximation for the effective diffusive flux as a function of the geometrical parameters, namely the film thickness, the support porosity and the pore size. We find a good agreement with full numerical solutions, and that a good effective rate is achievable with a relatively small number of pores.

Introduction. – Semi-permeable membranes provide a simple, robust and energy efficient basis for separation of mixtures, both liquid and gaseous, as well as energy conversion from salinity gradients [1–4]. State-of-the-art membranes used for such separation, and particularly for wastewater purification and seawater desalination, are polymeric composite structures comprised of an ultra-thin, selective film ($\sim$ 10–100 nm thick) cast over a porous membrane (see fig. 1 for an image and a schematic drawing of the support layer). This structure has proven to be a successful strategy for controlling the thin-film thickness without compromising the mechanical integrity of the overall membrane. In fact, the underlying membrane is commonly known as "the support", reflecting its assumed role in providing mechanical backing for the delicate thin film (often referred to as the "active" layer, since the separation is assumed to be controlled by it). However, recent studies have established the important role the support plays in dictating the overall transport properties of the composite structure. This is partially caused by the support structure's impact on the fabrication process through interfacial polymerization [5], but is primarily due to modification of diffusive transport at the film-support interface [6,7]; simply put, the solid fraction of the support obstructs transport, while the fluid-filled pores allow sig-

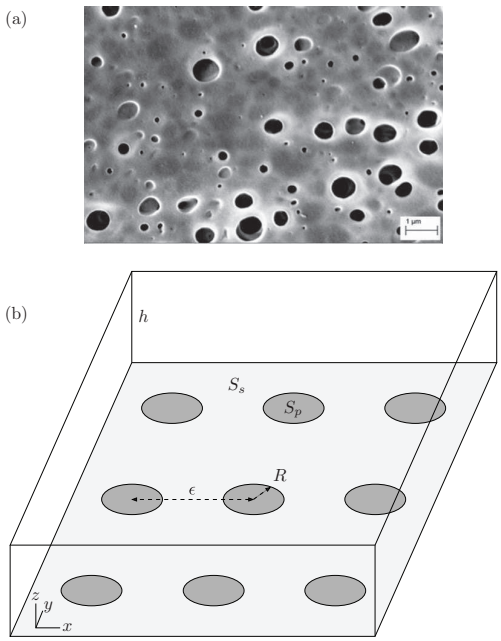

Fig. 1: (a) Scanning electron micrograph of a support membrane illustrating the porous structure (image reproduced from [8] with permission from Elsevier). (b) Schematic diagram of a portion of the composite membrane set-up considered, a top film membrane and a bottom support with a periodic array of pores.

(a) E-mail: bruna@maths.ox.ac.uk

nificantly higher mass transfer rates. Thus, transport is greatly influenced by the support surface morphology.

As shown in fig. 1(b), a particle diffusing through the selective film encounters a "patchy" interface with the support, with alternating solid and fluid areas. This type of configuration, where "reactive" patches are present on an otherwise inert surface, occurs in other processes, including microelectrode arrays [9] and chemoreceptors or protein ligands on the cell surface [10]. In most applications, the domain of diffusion is taken to be the infinite half-space, so that a constant concentration is prescribed far away from the patchy surface. This problem has been treated in [11] considering a periodic array of circular electrodes, and in [12] for irregular shapes in the limit of low surface cover. In the present context, however, the finite thickness of the domain is a main feature, and plays a major role in the function of the membrane. Previous studies have shown how the effective permeability of the membrane changes with the selective film thickness, as well as support pore size and porosity [13–15]. However, these results have mainly been obtained using numerical methods and, as such, provide limited physical insight.

Here we obtain simple analytical expressions for the effective transport properties of the composite structure, using matched asymptotic expansions. Our results are shown to compare very well with numerical calculations, and have the added benefit of identifying the key combination of geometrical parameters which determines the effective flux through the membrane.

Model. – We consider a composite membrane, comprising a top film of uniform thickness h overlaying a porous support layer, modelled as a periodic array of cylindrical pores, each of radius R, with separation of centres ϵ, as illustrated in fig. 1(b). The interface between the support layer and the thin film is taken to be $z = 0$, and the top surface of the film (in contact with the feed mixture) is therefore $z = h$. The top surfaces of the pores are denoted S_p, and the remaining solid, reflecting support region is denoted S_s. The diffusing species (of constant diffusion coefficient D) is assumed to be at a constant concentration c_∞ at the inlet/feed and to be removed from the system when in contact with a pore at $z = 0$.

Scaling length with h, time with h^2/D, and concentration with c_∞, the steady-state mass transport of the diffusive species in the membrane may be written in the dimensionless form

$$\nabla^2 c = 0, \tag{1a}$$

where $c(\mathbf{x})$ is the concentration and $\mathbf{x} = (x, y, z)$ denotes the position vector, together with boundary conditions

$$c = 0 \quad \text{on} \quad z = 0,\ \mathbf{x} \in S_p, \tag{1b}$$

$$\frac{\partial c}{\partial z} = 0 \quad \text{on} \quad z = 0,\ \mathbf{x} \in S_s, \tag{1c}$$

$$c = 1 \quad \text{on} \quad z = 1. \tag{1d}$$

The support surface at $z = 0$ now comprises a square array of periodic cells of size $\bar\epsilon \times \bar\epsilon$, with one circular pore of radius $\bar R$ at the center of each cell, where $\bar\epsilon = \epsilon/h$ and $\bar R = R/h$. The assumption of a perfect sink condition, *i.e.* $c = 0$ when the diffusing species reaches a pore at $z = 0$, should not be confused with an assumption of a perfectly selective membrane. We note also that the perfect sink assumption could be relaxed to consider a diffusive process within the pore, with diffusion coefficient $D_p \gg D$ (diffusion through the fluid-filled pore is much faster than through the solid material forming the thin, selective film). Here we consider the limit $D_p/D \to \infty$ so that a particle in S_p is instantly taken through the pore. The solid portions of the support are taken to be impermeable; again, this assumption could be relaxed to allow a small amount of diffusion in the solid.

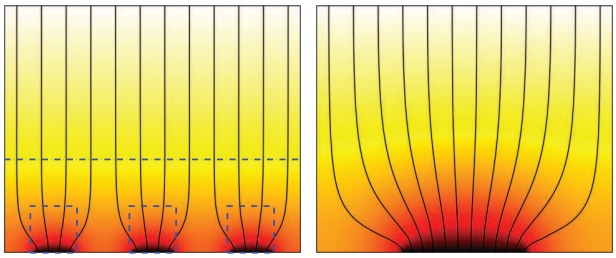

Fig. 2: (Color online) Concentration distribution c and streamlines of ∇c through plane $x = 0$ obtained solving (1) with (a) $\bar\epsilon = 0.4$ and $\bar R = 0.08$ and (b) $\bar\epsilon = 1.2$ and $\bar R = 0.24$. In (a), the dashed regions indicate the inner regions around each pore where $\mathbf{x} = O(\bar\epsilon^2)$, and the dot-dashed line indicates the boundary (at $\mathbf{x} = O(\bar\epsilon)$) between the intermediate and the outer regions. The colormap is the same in both plots.

Our goal is to determine the transport rate through the plane $z = 0$ as a function of the geometry, characterized by the parameters $\bar R$, $\bar\epsilon$ and h. Due to periodicity, we need only consider a single cell. We choose a coordinate system with origin at the center of the pore, so that the domain of diffusion is $\{(x, y, z) : |x| \le \bar\epsilon/2, |y| \le \bar\epsilon/2, 0 \le z \le 1\}$. We denote the bottom support surface at $z = 0$ by S; this contains now one single pore S_p in the center and support material $S_s = S \backslash S_p$. Since the flux is zero on the support matrix S_s, the average dimensionless flux is

$$Q = \frac{1}{\bar\epsilon^2} \int_S \frac{\partial c}{\partial z}\, \mathrm{d}S = \frac{1}{\bar\epsilon^2} \int_{S_p} \frac{\partial c}{\partial z}\, \mathrm{d}S. \tag{2}$$

Figure 2 shows the numerical solution of (1) for the concentration c, and the diffusive flux streamlines for two representative geometries, one with large pores ($\bar\epsilon = 2$ and $\bar R = 0.4$) and the other with small pores ($\bar\epsilon = 0.4$ and $\bar R = 0.08$). From these numerical solutions we could compute the flux (2) for various values of the parameters. However, this approach can provide only limited insight into the geometric effects in the problem. Instead, in this letter we approach the problem analytically, reducing the support layer to an effective boundary condition using the methods of multiple scales and matched asymptotic expansions.

When the pores are small, the streamlines plot (fig. 2(a)) shows that there is a boundary layer near the pore at $z = 0$ where the concentration field adapts to the heterogeneous base, while above this boundary layer the streamlines are vertical. In contrast, for the case with large pores (fig. 2(b)), this boundary layer spans the membrane film in its entirety. Here, we focus on the first case, because smaller pores in the support structure result in better, more mechanically robust membranes [16]. Thus, we consider the regime where $\bar{\epsilon} \ll 1$. As we will see later, this regime can still offer a remarkably good flux through the support layer. We will find that the distinguished limit corresponds to $\bar{R} = O(\bar{\epsilon}^2)$, so we set $\bar{R} = a\bar{\epsilon}^2$ with $a = O(1)$ as $\bar{\epsilon} \to 0$. We break the domain into three asymptotic regions: an *outer region* away from the support layer where $z = O(1)$, an *intermediate region* where $\mathbf{x} = O(\bar{\epsilon})$, and an *inner region* near the pore where $\mathbf{x} = O(\bar{\epsilon}^2)$ (see fig. 2(a)). The intermediate and inner regions which follow are essentially equivalent to those considered in [12], though they did not match them to the outer region, which allows us to consider a finite membrane thickness.

Outer region. Outside the boundary layer the diffusing particles see a homogenized boundary with condition

$$\frac{\partial c}{\partial z} = kc \qquad \text{on} \qquad z = 0, \tag{3}$$

where k (which depends on $\bar{\epsilon}$ and a) is the effective removal rate, which we aim to determine. The solution in the outer region is then simply

$$c = 1 + \frac{k(z-1)}{1+k}. \tag{4}$$

Intermediate layer. In the boundary layer region near $z = 0$ we rescale $\mathbf{x} = \bar{\epsilon}\mathbf{X}$ and write $c(\mathbf{x}) = \hat{c}(\mathbf{X})$. In this region the pore appears as a point sink. By symmetry, we can replace the periodic boundary conditions on the sides of the cell, $S_{\text{sides}} = \{Z > 0, |X| = 1/2 \text{ or } |Y| = 1/2\}$, with no-flux boundary conditions. Then $\hat{c}(\mathbf{X})$ satisfies

$$\hat{\nabla}^2 \hat{c} = 0, \qquad Z > 0, \tag{5a}$$

$$\hat{\nabla}\hat{c} \cdot \hat{\mathbf{n}} = 0, \qquad \mathbf{X} \in S_{\text{sides}}, \tag{5b}$$

$$\frac{\partial \hat{c}}{\partial Z} = \alpha\delta(X,Y), \qquad Z = 0, \tag{5c}$$

where $\mathbf{n}$ is the outward unit normal and δ is the Dirac delta function, with $\hat{c}$ matching with c as $Z \to \infty$. Here $\alpha = \alpha(\bar{\epsilon})$ represents the (as yet unknown) strength of the sink. Integrating $\hat{c}$ over the periodic cell gives

$$\int_{Z=0} \frac{\partial \hat{c}}{\partial Z} \mathrm{d}X\mathrm{d}Y = \int_{Z=\infty} \frac{\partial \hat{c}}{\partial Z} \mathrm{d}X\mathrm{d}Y. \tag{6}$$

Matching with the outer solution gives

$$\frac{\partial \hat{c}}{\partial Z} \sim \bar{\epsilon}\frac{\mathrm{d}c}{\mathrm{d}z}(0)Z \qquad \text{as} \qquad Z \to \infty \tag{7}$$

to all orders in $\bar{\epsilon}$. Using (7) and (5c) in (6) gives

$$\alpha = \bar{\epsilon}\frac{\mathrm{d}c}{\mathrm{d}z}(0). \tag{8}$$

To solve for $\hat{c}$, we note that, to all orders in $\bar{\epsilon}$,

$$\hat{c} = c(0) + \alpha u, \tag{9}$$

where u satisfies

$$\begin{aligned} \hat{\nabla}^2 u &= 0, && Z > 0, \\ \hat{\nabla} u \cdot \hat{\mathbf{n}} &= 0, && Z > 0, (X,Y) \in S_{\text{sides}}, \\ \frac{\partial u}{\partial Z} &= \delta(X,Y), && Z = 0, \\ u &\sim Z, && Z \to \infty. \end{aligned} \tag{10}$$

In turn, the solution to (10) can be written as

$$u = -\frac{1}{2\pi\|\mathbf{X}\|} + G, \tag{11}$$

where G is regular and does not depend on any parameters; G can be obtained as an infinite series [12] or solved for numerically (see appendix).

Inner region. Finally, we rescale onto the scale of the pore by setting $\mathbf{x} = \bar{\epsilon}^2\boldsymbol{\xi}$ with $\boldsymbol{\xi} = \{\xi, \eta, \zeta\}$ and writing $c(\mathbf{x}) = \tilde{c}(\boldsymbol{\xi})$. On this scale the domain of diffusion is the half-space $\zeta > 0$. We find

$$\begin{aligned} \tilde{\nabla}^2 \tilde{c} &= 0, && \zeta > 0, \\ \frac{\partial \tilde{c}}{\partial \zeta} &= 0, && \zeta = 0, \quad r \equiv \sqrt{\xi^2 + \eta^2} > a, \\ \tilde{c} &= 0, && \zeta = 0, \quad r \le a, \end{aligned} \tag{12}$$

with solution (see [17])

$$\tilde{c} = A - \frac{2A}{\pi} \arcsin\left[\frac{2a}{\sqrt{\zeta^2 + (a+r)^2} + \sqrt{\zeta^2 + (a-r)^2}}\right], \tag{13}$$

valid for $\zeta > 0$. The constant A will be determined by matching. Writing $\tilde{c}$ in terms of the intermediate variable $\mathbf{X}$ and expanding gives

$$\tilde{c} = A - \frac{2\bar{\epsilon}aA}{\pi\|\mathbf{X}\|} + O(\bar{\epsilon}^2). \tag{14}$$

On the other hand, as $\|\mathbf{X}\| \to 0$,

$$\hat{c} \sim c(0) + \alpha\left(\frac{-1}{2\pi\|\mathbf{X}\|} + G(\mathbf{0})\right). \tag{15}$$

Matching the regular parts of (14) and (15) first leads to

$$A = c_0(0) + \alpha G(\mathbf{0}). \tag{16}$$

Matching the singular terms gives

$$\alpha = 4a\bar{\epsilon}A. \tag{17}$$

Eliminating α and A from (8), (16) and (17) gives

$$\frac{\mathrm{d}c}{\mathrm{d}z}(0) = \frac{4a}{1 - 4a\bar{\epsilon}G(0)}\, c(0). \tag{18}$$

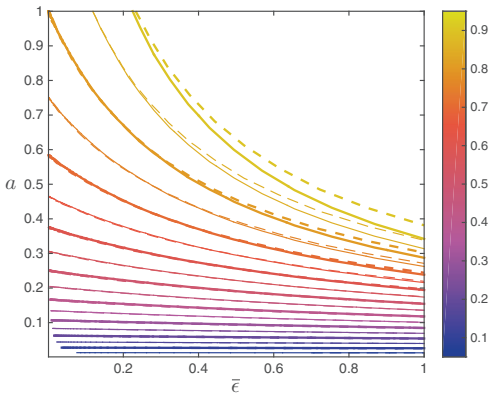

Fig. 3: (Color online) Flux per unit area Q as a function of the relative pore size a and the pore separation $\bar{\epsilon}$, computed from (2) using the full numerical solution (dashed lines) and from the asymptotic result (20) (solid lines).

Comparing with (3) we see that the effective removal rate

$$k = \frac{4a}{1 - 4a\bar{\epsilon}G(\mathbf{0})}, \tag{19}$$

which agrees with the results in [12]. Numerically we find that $G(\mathbf{0}) \approx 0.6207$ (see appendix). With k determined, we can now use (4) to compute the average flux through the membrane as

$$Q \equiv \frac{\mathrm{d}c}{\mathrm{d}z}(0) = \frac{4a}{1 + 4a - 4a\bar{\epsilon}G(\mathbf{0})}. \tag{20}$$

We have been working in nondimensional variables throughout. If we redimensionalise we find that the Robin boundary condition (3) becomes

$$D\frac{\partial c}{\partial z} = Kc \qquad \text{on} \qquad z = 0, \tag{21}$$

where

$$K = \frac{Dk}{h} = \frac{4RD}{\epsilon^2 - 4R\epsilon G(\mathbf{0})}, \tag{22}$$

where we recall that R is the pore radius and ϵ is the separation of pore centres. Note that K depends on the support geometry only, and is independent of the thickness of the selective film, h. The dimensional flux through the membrane is

$$D\frac{\mathrm{d}c}{\mathrm{d}z}(0) = \frac{4RDc_\infty}{\epsilon^2 + 4hR - 4R\epsilon G(\mathbf{0})}. \tag{23}$$

Results. – The average flux Q of the solution to (1) evaluated via (2), is compared in fig. 3 with the asymptotic result in (20). We observe that the asymptotic expression agrees qualitatively with the numerical solution, and that the quantitative agreement is very good in the parameter region expected from the asymptotic analysis, namely when $\bar{\epsilon} \ll 1$ and $a \ll 1$.

In the previous plot we varied the relative pore size a and the pore spacing $\bar{\epsilon}$ independently. If the porosity of the support layer $\phi = \pi\bar{R}^2/\bar{\epsilon}^2$, is kept constant, we find that the flux increases with the pores separation $\bar{\epsilon}$ (fig. 4(a)).

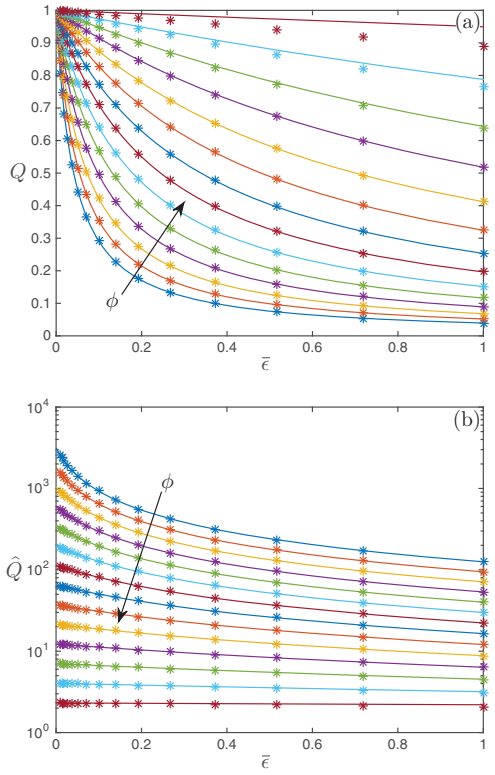

Fig. 4: (Color online) (a) Comparison of the exact (data points) and homogenized (solid lines) flux Q as a function of the pore separation $\bar{\epsilon}$ for a constant porosity $\phi = \pi\bar{R}^2/\bar{\epsilon}^2$. (b) Flux per unit of pore area, $\widehat{Q} = Q\bar{\epsilon}^2/(\pi\bar{R}^2)$ (log scale). In both plots, each line corresponds to a different ϕ, taking values $\phi = 0.0003$, 0.0005, 0.0010, 0.0017, 0.0029, 0.0051, 0.0088, 0.0154, 0.0268, 0.0468, 0.0816, 0.1422, 0.2479, and 0.4322.

This is consistent with the result that, for two isolated pores, the maximum flux occurs as the pore separation goes to infinity [18]. On the other hand, for a fixed pore separation $\bar{\epsilon}$ a higher porosity clearly leads to a higher flux, though this may result in a mechanically weaker composite. Figure 4(a) shows the flux Q per unit of pore area $\pi\bar{R}^2$. In this plot we see that there are "diminishing returns" in increasing porosity to give a higher flux.

Another interesting scenario is to consider how the flux varies for a constant pore radius $\bar{R}$ (fig. 5). In this case, for a fixed $\bar{R}$ the flux per unit area Q increases as the pores come closer ($\bar{\epsilon}$ decreasing). The discrepancy between the theoretical and numerical Q can only be seen for relatively large pore sizes as we approach the maximum pore size, attained when $\bar{R} = \bar{\epsilon}/2$.

Discussion. – We have studied the homogenization problem of a composite membrane with a periodic nonuniform support layer. We find that the support layer can be modelled by an effective Robin boundary condition (21). The removal rate K, given in (22), depends on the geometrical parameters of the support, namely the separation between pores ϵ and the pore radius R, the pore radius. However, it does not depend on the thickness of the selective film, h.

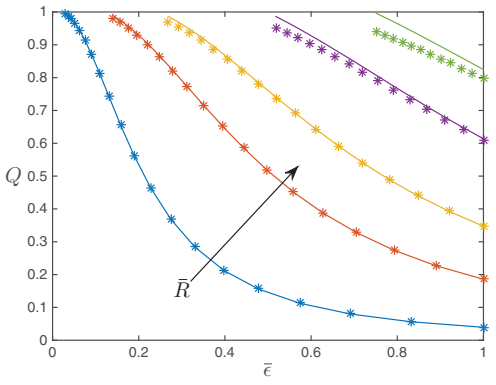

Fig. 5: (Color online) Comparison of the exact (data points) and homogenized (solid lines) flux Q as a function of $\bar{\epsilon}$ for a constant pore radius $\bar{R}$. The five lines correspond to radius $\bar{R} = 0.01$, 0.05, 0.1, 0.2, and 0.3 with the arrow indicating the direction of increasing $\bar{R}$.

The limiting case $k = Kh/D \to 0$ corresponds to a perfectly reflecting support layer, while the limiting case $k \to \infty$ corresponds to a perfectly absorbing support layer. The latter is the "perfect" support layer. This may be counterintuitive in a membrane application, as we want membranes to inhibit solutes passing through, but one must recall that the purpose of the support layer is to give mechanical support to the selective ultra-thin film, and hence the more invisible it is to transport, the better. At leading order the nondimensional rate k given by (19) is $O(Rh/\epsilon^2)$. This implies that the pore size needed to achieve a sizeable flux through the composite membrane is $O(\epsilon^2/h)$ which can be much smaller than the pore separation when $\epsilon \ll h$. For example, a pore radius $R = 2\epsilon^2/h$ gives a flux 89% of that of a perfect support, with a surface porosity of only $\phi = 4\pi\epsilon^2/h^2$. This implies that, in this asymptotic regime, the support membrane would be mechanically very good, while also having a good permeability.

We can look at this conclusion in a broader perspective. For example, in the context of biological cell receptors, this explains why the cellular membrane can accommodate many specialized receptors, each adsorbing molecules of a specific kind with an efficiency of the same order as that of a fully covered surface [10] (Chapt. 2, p. 30). A similar problem was considered in [11], in the context of microelectrodes. They considered a membrane of infinite thickness (solution in the infinite half-space $z > 0$), allowing for bulk regeneration (nonzero right-hand side in eq. (1a)) and for surface oxidation (Robin boundary condition instead of (1b) on the electrodes). They found that, in the parameter regime where both surface electrode and bulk reactions are switched off, their solution breaks down. This corresponds to the solution presented here in the limit of $\bar{\epsilon} \to 0$. By splitting the domain into three regions (inner, intermediate and outer) we were able to compute the rate at which the average flux, given by (20), goes to zero.

An important assumption in our model is that the solute and solvent diffusion through the thin polymeric film is decoupled, so that the effective rate analysis applies equally to both species. This assumption has been shown to be consistent with experimental observations and holds true, thermodynamically, for the low fluxes encountered in practice. In water purification processes, the quality of a membrane is measured by its permeability, *i.e.* the effective flux per unit driving force (here embodied by K), and its solute rejection, defined as $\mathcal{R} = (1 + K_s/Q_w)^{-1}$, where Q_w is the water flux and K_s the salt permeability [16]. While all species diffuse across the membrane, a high rejection reflects the much faster transport of the preferred species (water, say). However, in practice, the water flux may be controlled by an applied pressure (as is the case for reverse osmosis), while the solute transport remains unaffected by it. At a fixed water flux, variations of the permeability due to the support will be reflected solely in the solute transport. Using our asymptotic expression for the permeability, at leading order by (20), we have $\mathcal{R} \sim (1 + \phi/R)^{-1}$, which shows that rejection will increase for larger pores at constant porosity; conversely, at fixed pore size, rejection will decrease with increased porosity. These inverted trends have been shown numerically in [6] but are here revealed directly in our asymptotics. The implication is that one may tune the rejection/permeability trade-off of a membrane through manipulation of support morphology, offering an extra degree of freedom, beyond the structure and chemistry of the "active" layer.

Here we considered an idealized support with a periodic square array of pores. It is natural to ask how the results change with the way the pores (or electrodes, or cell receptors, ...) are distributed. This question was addressed in [12] and [19] by considering irregular pore shapes or a random uniform distribution of pores, respectively. In [12] they considered the limit of low porosity and found that the effect of the pore shape only comes at order a^4 in (19). The problem of two isolated pores was solved analytically by Sneddon in [18], who found that the flux increased with the pore separation, the best flux occurring when the pores are so far apart that they do no longer interact with each other. This implies that, for a desired surface cover ϕ, the best possible distribution would be a periodic array (in fact hexagonal rather than square), so that the separation between any two pores is maximized. Thus, an interesting question is whether a hexagonal array indeed gives a better flux Q than a square array. On the other hand, for two isolated pores the greatest reduction is 74% of the perfect flux, and is achieved when the two pores are in contact [18]. Therefore, the deviation from perfection is rather small. This suggests that for multiple pores, while support layer pore periodicity offers the best properties, one with an equal surface porosity ϕ but a random pore distribution would not be "too far off". If manufacturing complexity and cost come into the equation, this would suggest that "not perfect" periodic support layers may be preferable.

When considering the importance of the pore arrangement in the support layer, we stress that our asymptotic

solution shows that relatively very small pores and, hence, very small surface porosity ϕ, are sufficient. In the case of a random pore distribution, such conditions would imply a low likelihood of pores clustering together, so that well-separated pores can be assumed. Therefore, this would hint towards the conjecture that pore distribution is unimportant in the range of surface porosities relevant to this application.

In this work we have assumed that the support layer had two regions, one of perfectly absorbing pores S_p and another of perfectly reflecting support S_s. An obvious extension would be to relax these conditions, and consider a support with a small absorption rate, or pores that are not perfect sinks. The latter case would be more realistic since even when a particle reaches a pore, there is a chance that it is not removed from the system.

Finally, while we have considered a flat patchy surface, the results presented here can be extended in a relative straightforward way to nonplanar surfaces encountered in many applications, such as cell receptors.

Appendix

We look for a solution to (10) of the form $u = s + G$, where s is the *singular part* and takes care of the sink at $\mathbf{X} = \mathbf{X}_0 = \mathbf{0}$ and G is the *regular part*. In order to solve for s, it is convenient to "move" the singularity from the boundary condition to the right-hand side of the equation, and write

$$\begin{aligned} \hat{\nabla}^2 s(\mathbf{X}, \mathbf{X}_0) &= \delta(\mathbf{X} - \mathbf{X}_0), & Z > 0, \\ \frac{\partial s}{\partial Z} &= 0, & Z = 0. \end{aligned}$$

With the method of images, the solution is $s(\mathbf{X}, \mathbf{X}_0) = -\Gamma(\mathbf{X} - \mathbf{X}_0) - \Gamma(\mathbf{X} - \mathbf{X}_0^*)$, where $\mathbf{X}_0^*$ is the image point, $\mathbf{X}_0^* = (X_0, Y_0, -Z_0)$, and Γ is Laplace's fundamental solution, $\Gamma = 1/(4\pi\|\mathbf{X}\|)$. Setting $\mathbf{X}_0 = \mathbf{0}$ we find that

$$s(\mathbf{X}) = -\frac{1}{2\pi\|\mathbf{X}\|}. \tag{A.1}$$

Using (A.1), the regular part G satisfies the following problem:

$$\begin{aligned} \hat{\nabla}^2 G &= 0, & Z > 0, \\ \hat{\nabla} G \cdot \hat{\mathbf{n}} &= \hat{\nabla}\left(\frac{1}{2\pi\|\mathbf{X}\|}\right) \cdot \hat{\mathbf{n}}, & Z > 0, (X, Y) \in S_{\text{sides}}, \\ \hat{\nabla} G \cdot \hat{\mathbf{n}} &= 0, & Z = 0, \\ G &\to Z, & Z \to \infty. \end{aligned} \tag{A.2}$$

In the expression of the homogenized rate (19) and homogenized flux (20) we only need the value of G at the origin. We compute the value of $G(\mathbf{0})$ by writing $G = Z + \hat{G}$ and solving for $\hat{G}$ numerically (replacing the boundary condition on $Z = 0$ in (A.2) by $\hat{\nabla}\hat{G} \cdot \hat{\mathbf{n}} = 1$ and the condition at infinity by $\hat{G} \to 0$). The infinite domain is approximated by a finite prism of height L, and we obtain $G(\mathbf{0})$ up to 4 digits of accuracy with a Richardson extrapolation using repeated solutions $\hat{G}$ in domains of height $L = 10,\ 20,\ \ldots, 200$. We find $G(\mathbf{0}) = 0.6207$.

* * *

We are grateful to Ian Griffiths and Howard Stone for organizing the Oxford-Princeton Workshop that triggered this collaboration, as well as to Christopher Bell for valuable discussions. MB is partially supported by the EPSRC (EP/I017909/1). GZR was supported through a Marie-Curie IOF (grant No. 275911) under the FP7 programme of the European Research Council.

REFERENCES

[1] Shannon M. A., Bohn P. W., Elimelech M., Georgiadis J. G., Mariñas B. J. and Mayes A. M., *Nature*, **452** (2008) 301.
[2] Saxena A., Tripathi B. P., Kumar M. and Shahi V. K., *Adv. Colloid Interface Sci.*, **145** (2009) 1.
[3] Du N., Park H. B., Robertson G. P., Dal-Cin M. M., Visser T., Scoles L. and Guiver M. D., *Nat. Mater.*, **10** (2011) 372.
[4] Elimelech M. and Phillip W. A., *Science*, **333** (2011) 712.
[5] Ghosh A. K. and Hoek E. M. V., *J. Membrane Sci.*, **336** (2009) 140.
[6] Ramon G. Z., Wong M. C. and Hoek E., *J. Membrane Sci.*, **415** (2012) 298.
[7] Ramon G. Z. and Hoek E., *J. Membrane Sci.*, **425** (2013) 141.
[8] Wei J., Qiu C., Tang C. Y., Wang R. and Fane A. G., *J. Membrane Sci.*, **372** (2011) 292.
[9] Huang X. J., O'Mahony A. M. and Compton R. G., *Small*, **5** (2009) 776.
[10] Berg H. C., *Random Walks in Biology* (Princeton University Press) 1993.
[11] Lucas S. K., Sipcic R. and Stone H. A., *SIAM J. Appl. Math.*, (1997).
[12] Belyaev A. G., Chechkin G. A. and Gadyl'shin R. R., *SIAM J. Appl. Math.*, **60** (1999) 84.
[13] Davis A. M. J. and Ethier C. R., *Chem. Eng. Sci.*, **48** (1993) 1655.
[14] Ethier C. R. and Kamm R. D., *J. Membrane Sci.*, **43** (1989) 19.
[15] Lonsdale H. K., Riley R. L., Lyons C. R. and Carosella D. P., *Transport in Composite Reverse Osmosis Membranes*, in *Membrane Processes in Industry and Biomedicine*, edited by Bier M. (Plenum Press, New York) 1971, pp. 101–122.
[16] Strathmann H., *Introduction to Membrane Science and Technology*, Vol. **51** (Wiley) 2012.
[17] Crank J. and Furzeland R. M., *IMA J. Appl. Math.*, **20** (1977) 355.
[18] Sneddon I. N., *Mixed Boundary Value Problems in Potential Theory* (North-Holland, Amsterdam) 1966.
[19] Berezhkovskii A. M., Makhnovskii Y. A., Monine M. I., Zitserman V. Y. and Shvartsman S. Y., *J. Chem. Phys.*, **121** (2004) 11390.